Anisotropic Frequency-Dependent Spreading of Seismic Waves from VSP Data Analysis

Amin Baharvand Ahmadi* and Igor Morozov, University of Saskatchewan, Saskatoon, Saskatchewan
amin.baharvand@usask.ca

GeoConvention 2012:Vision

Summary

A model combining geometrical spreading, scattering, and effects of attenuation (*Q*) is derived from first-arrivals amplitudes in a multi-offset VSP dataset. The inversion reveals variations of geometrical attenuation (wavefront curvatures and scattering) and the effective *Q* with depth. Both of these properties are also found to be anisotropic. The resulting model of frequency-dependent amplitudes correctly predicts the field data and should be useful for true-amplitude studies, including inversion, *Q*-compensation, and AVO analysis.

Introduction

Accurate corrections for geometrical spreading and attenuation are important for seismic studies relying on amplitudes, such as true-amplitude imaging, inversion, *Q*-compensation, or analysis of amplitude variations with offset (AVO). Usually, such corrections are based on simple empirical relations for amplitudes, such as:

$$A \propto R^{-\alpha} \exp\left(-\pi f t/Q\right) , \tag{1}$$

where R is the source-receiver distance, t is the travel time, f is the frequency, α is the geometrical-spreading exponent, and Q is the quality factor. Such expressions work well in areas where the geometrical spreading is close to the theoretical limit ($\alpha \approx 1$) and $Q^{-1} \ll 1$. However, in many practical cases, amplitudes decay much faster than prescribed by this law, with α reaching or even exceeding ~2 (Hardage, 1985). In such cases, the power-law form of the geometrical-spreading factor in (1) is unlikely accurate, and Q^{-1} trades off with α. Errors in the values of α and other uncertainties in geometrical spreading lead to uncertainties and spurious frequency dependences in Q, which may present significant difficulties for modeling and interpretation (Morozov, 2008, 2010).

Vertical seismic profiles (VSP) provide the most complete information about the variations of seismic amplitudes with depths and propagation directions. Because of this, VSP offers the best opportunity for detailed analysis of geometrical spreading and attenuation. Here, we use an 80-level three-component VSP dataset acquired in 1999 as part of the Weyburn-Midale CO_2 Monitoring and Storage Project in southern Saskatchewan, Canada, to invert for combined geometrical and *Q*-related attenuation. Only vertical components of first-arrival recordings from multiple shots are used in the following analysis.

Data and Method

Instead of (1), we describe both the geometrical spreading and attenuation by using frequency-dependent attenuation coefficients accumulated along the rays (Morozov, 2008):

$$u = \frac{A_R A_S}{R} \exp\left[-\int_{\text{Ray}} \left(\gamma + f\kappa\right) dt \right] , \tag{2}$$

where A_R and A_S are the source and receiver factors, $1/R$ is the "background" spherical-wave geometrical spreading, and γ and κ describe the frequency-independent and frequency-dependent parts of the attenuation coefficient. Parameter γ can be associated with geometrical spreading and scattering, and parameter κ is related to the "effective" Q_e of the medium as $\kappa = \pi/Q_e$ (Morozov, 2010, 2011). From the analysis of VSP data (below), it is also apparent that the amplitude decay depends on the directions of propagation. Therefore, in (2), we use anisotropic values of γ and κ, parameterized as follows:

$$\gamma = \gamma_1\left(1+\theta\sin^2\varphi\right) \text{ , and } \kappa = \kappa_1\left(1+\beta\sin^2\varphi\right), \tag{3}$$

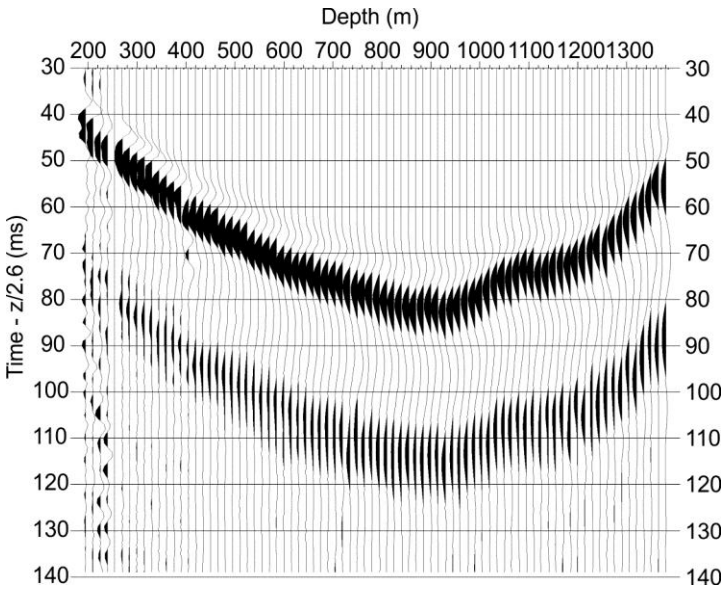

Figure 1: Vertical-component records from a near-offset VSP shot. Linear moveout of 2.6 km/s was applied in order to zoom in on the first arrivals.

where φ is the propagation angle relative to the downward vertical direction, γ_1 and k_1 are the "geometrical" and frequency-dependent attenuation parameters in the vertical direction, and θ and β are the corresponding anisotropy parameters. From (3), the "horizontal" attenuation parameters are $\gamma_2 = \gamma_1(1+\theta)$ and $\kappa_2 = \kappa_1(1+\beta)$.

To invert for the attenuation parameters for the study area, we picked the first-arrival travel times and amplitudes from 35 vertical-component VSP shot records (Figure 1). Multiple amplitudes were picked from records filtered within narrow frequency bands centered from 10 to 150 Hz.

Using the first-arrival travel times, we constructed a six-layer interval velocity model (Figure 2). To each layer, a combination of parameters γ_1, κ_1, θ, and β was assigned. Rays were traced by using straight segments within each layer (Figure 2). To remove the effects of source amplitudes and emphasize those of spreading, logarithms of spectral ratios of the amplitudes in eq. (2) were calculated for pairs of receivers within each shot:

$$A_{12} \equiv \ln\frac{u_1/\left(A_R A_S/R\right)_1}{u_2/\left(A_R A_S/R\right)_2} = -\sum_{i=1}^{N_{layers}}\left(\gamma_i + f\kappa_i\right)\left(t_i^1 - t_i^2\right) \text{ ,} \tag{4}$$

where subscripts and superscripts 1 and 2 indicate the receivers, subscripts i are layer numbers, and t_i^k denotes the travel time within i-th layer to k-th receiver. To form these receiver pairs, we used receivers located near the bottom of each layers and a common reference receiver at the top of the downhole receiver spread (for example, blue and red rays in Figure 2).

To invert equations (4), a layer-stripping method appears to be the most convenient and reliable. This method also allows a layer-by-layer, visual control of the results. For layer k, eq. (4) can be written as:

$$\tilde{A}_{12} \equiv \frac{1}{t_i^2 - t_i^1}\left[A_{12} - \sum_{i=1}^{k-1}\left(\gamma_i + f\kappa_i\right)\left(t_i^1 - t_i^2\right)\right] - \left(\gamma_{1,k}\theta + f\kappa_{1,k}\beta\right)\sin^2\varphi = \gamma_{1,k} + f\kappa_{1,k} \text{ .} \tag{5}$$

The left-hand side in this equation is the spectral ratio corrected for the effect of the overlaying layers, travel-time differences, and anisotropy. As a result of these corrections, a simple linear dependence on

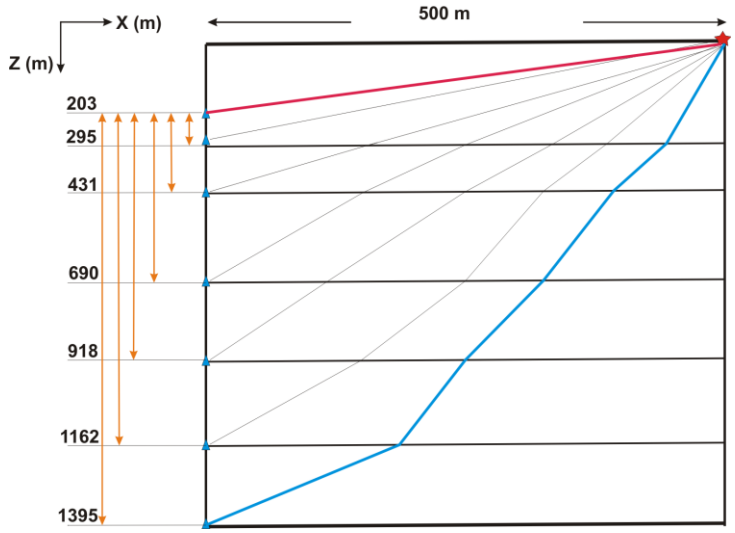

Figure 2: Depth model schematically showing rays traced from a shot to the geophones at different depths. Orange arrows indicate pairs of geophones used for measuring the attenuation parameters of each layer.

frequency can be observed. By iteratively adjusting the values of θ an β and picking $\gamma_{1,k}$ and $\kappa_{1,k}$ as the intercept and slope in the $\left(f, \tilde{A}_{12}\right)$ plane, attenuation parameters for layer k are obtained.

Results

Figure 3 illustrates the need for anisotropic attenuation parameters in eq. (3). Without anisotropy, the corrected spectral ratios in layer number 2 show significant systematic variations with variable source-borehole offsets (Figure 3a). These variations are reduced by using non-zero values of θ and β (Figure 3b). The resulting attenuation model is shown in Table 1. Data fits using the layer-stripping procedure are shown for several upper layers of the model in Figure 4. Note that despite some residual misfits, the values of γ_1 and κ_1 can be reliably constrained from these plots.

The resulting model shows negative values of γ_1 to ~430-m depths. Overall, the frequency-dependent effect ($f\kappa$) on seismic amplitudes at f = 10–150 Hz is significantly stronger than that of "geometrical attenuation" (γ, which includes scattering). Nevertheless, everywhere in the model, geometrical attenuation is much stronger than the levels of ~0.01 s^{-1} observed in crustal-scale studies (Morozov, 2008, 2010). Anisotropy is also the strongest within the upper part of the model to ~430-m depths. The values of geometrical attenuation anisotropy (θ) are around 2,showing significant anisotropy for vertical and horizontal directions. Parameters β are mostly in the range of ~0.2, which shows that the anisotropy in κ (and Q_e) values is moderate in the study area. The effective attenuation quality factors Q_e are 27 from the surface to ~430-m depths, increasing to 50 between 430 and 920-m and reaching 60 between 1160 and 1400-m depth (Table 1).

By using eqs. (2) and (3) with the layered model derived from first-arrival inversion (Figure 2; Table 1), we obtain a model for frequency-dependent seismic spreading in the study area. We tested our model on a near-offset VSP shot record and predicted the amplitude of first arrival by using 0-, 100- and 45-Hz frequencies. The low- and high-frequency curves show the range of spreading variations with frequency. As expected, the lowest attenuation is observed for zero frequency, and the amplitude decay rate increases with frequency. Using the dominant frequency of the record (45 Hz) predicts the first arrival amplitude of shot correctly (Figure 5). This model accurately (within the definition of our six-layer structure) predicts the amplitudes and attenuation properties of direct waves, and therefore it should be advantageous for any true-amplitude studies. Computationally, this model is still relatively simple, and it offers a definite advantage of empirical accuracy and agreement with the first arrivals within the entire frequency band.

Conclusions

A model combining geometrical spreading, scattering, and the effects of attenuation (Q) is proposed and inverted for by using first arrivals from a multi-offset VSP dataset. First-arrival amplitude data show that both geometrical attenuation (wavefront curvatures and scattering) and the effective Q are anisotropic.

Application of the resulting model for Weyburn VSP area allows predicting the amplitudes of the first arrivals correctly. Similarly, it could likely be used to correct complex spreading behavior for reflected

and converted waves. The resulting empirical, frequency-dependent, anisotropic model of amplitudes should be useful for many true-amplitude studies, including inversion, *Q*-compensation, and AVO analysis.

Acknowledgements

This study was part of Phase II of IEA GHG Weyburn CO_2 Storage and Monitoring Project.

References

Hardage, B. A., 1985, Vertical seismic profiling part A: principles: second enlarged edition, London, Geophysical Press, v. 14, 509 p, 172-172.

Morozov, I. B., 2008, Geometrical attenuation, frequency dependence of *Q*, and the absorption band problem, Geophys. J. Int. 175, 239–252.

Morozov, I. B., 2010, On the causes of frequency-dependent apparent seismological *Q*. Pure Appl. Geophys. 167, 1131–1146, doi 10.1007/s00024-010-0100-6.

Morozov, I. B., 2011, Mechanisms of geometrical attenuation. Ann. Geophys. 54, 235–248, doi: 10.4401/ag-4780.

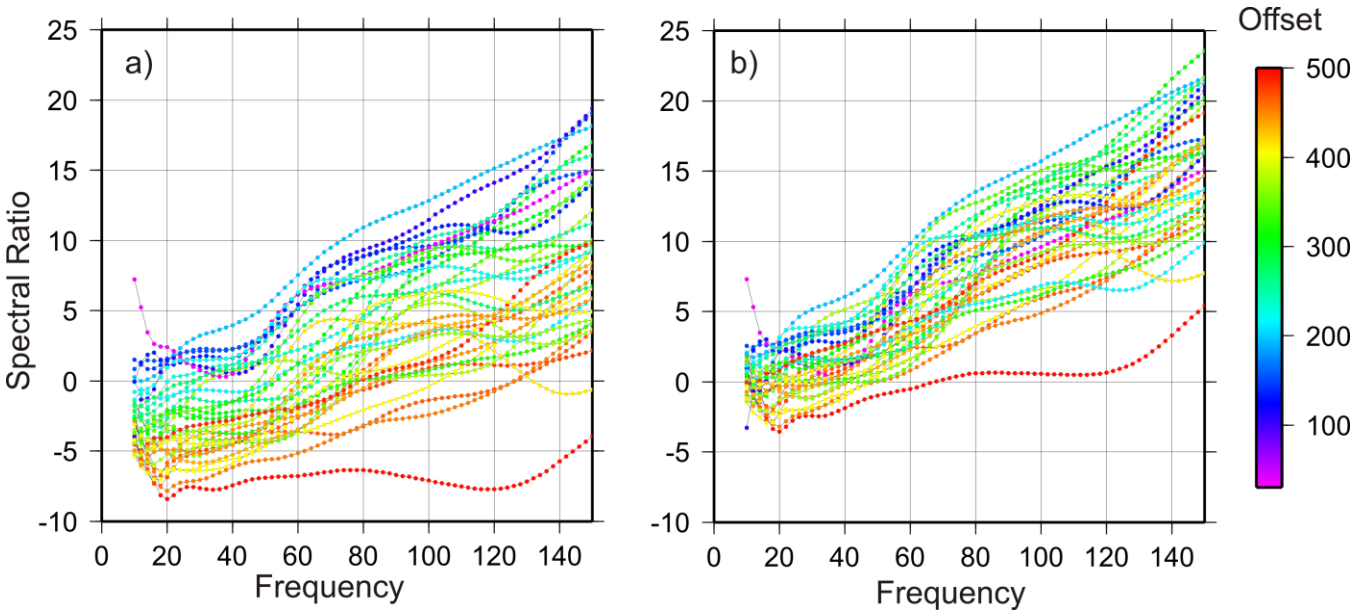

Figure 3: Effect of anisotropy: a) Fitting expression (5) for layer 2 by using $\theta = \beta = 0$, b) The same using anisotropic parameters. Note the significant systematic variations with variable source-borehole offsets in plot a), which are reduced by applying the geometrical anisotropy corrections (eq. (3))

Table 1: Resulting anisotropic attenuation model.

Layer	Depth (bottom)	γ (s^{-1})	κ	θ	β	$Q_e=\pi/\kappa$
1	295	-2	0.12	0*	0*	27
2	431	-2.2	0.12	2.6	-0.4	27
3	690	1.2	0.06	-1.8	-0.2	52
4	918	-1.5	0.06	1.8	0.2	52
5	1162	3.1	0.053	-1.55	0.2	59
6	1395	7.5	0.05	-1.85	0.2	63

* Not measured for layer 1

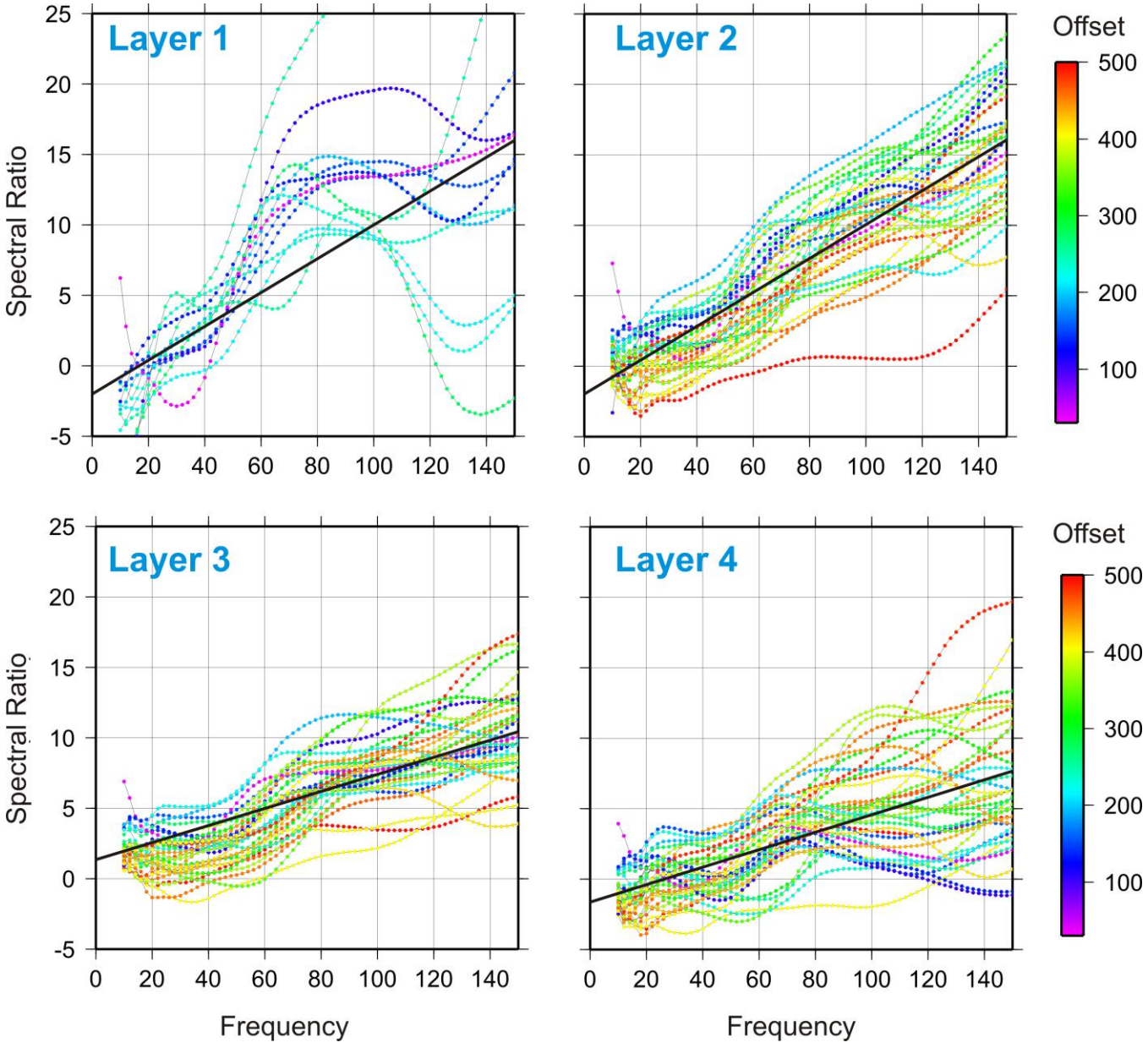

Figure 4: Corrected spectral ratios used to measure $\gamma_{1,k}$ and $\kappa_{1,k}$ by layer-stripping. Black lines indicate the inverted model parameters $\gamma_{1,k}$ and $\kappa_{1,k}$.

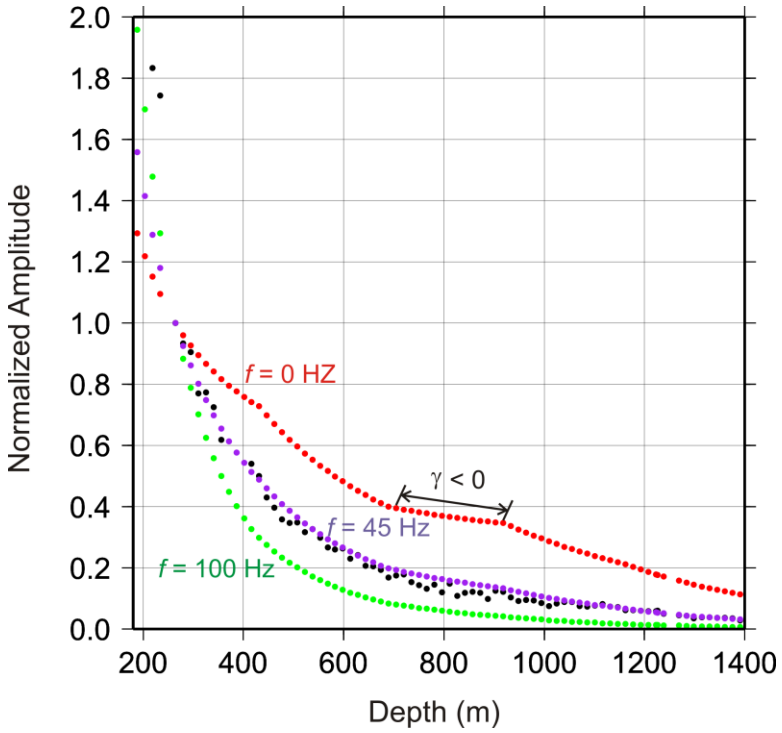

Figure 5: Combined geometrical spreading/scattering and frequency-dependent attenuation predicted by the model in Figure 2 and Table 1. Amplitudes normalized at 260-m depth. Black points indicate first-arrival amplitudes from one VSP shot (FFID 276), colored points denote predicted amplitude by the model at frequencies 0, 100 and 45 Hz. Note that the model predicts the first-arrival amplitudes correctly at the dominant frequency of 45 Hz (purple). Also note that the negative γ value in layer 4 affects the shape of the zero frequency amplitude by the model.